MOLECULAR REPRODUCTION AND DEVELOPMENT 73:1491–1502 (2006)

Transcriptome Profiling of the Tubular Porcine Conceptus Identifies the Differential Regulation of Growth and Developmentally Associated Genes

LE ANN BLOMBERG,[1]* WESLEY M. GARRETT,[1] MICHEL GUILLOMOT,[3] JEREMY R. MILES,[1] TAD S. SONSTEGARD,[2] CURTIS P. VAN TASSELL,[2] AND KURT A. ZUELKE[1]

[1]*Biotechnology and Germplasm Laboratory, USDA Agricultural Research Service, Beltsville, MD*
[2]*Bovine Functional Genomics Laboratory, USDA Agricultural Research Service, Beltsville, MD*
[3]*JMR Biologie du Développement et Reproduction, Institut National de la Recherche Agronomique, Jouy-en-Josas, France*

ABSTRACT Gastrulation and trophectoderm elongation of the porcine conceptus coincide with peak conceptus estrogen secretion from gestational day 11 to day 12. The current study aim was to identify genes required for elongation by defining the transcriptome profile of this dynamic tubular stage. The gastrulation and proliferative status of ovoid, tubular, and filamentous conceptuses were also examined. Polarization of the embryonic disc and growth throughout the conceptus were evident. An unamplified and two distinct amplified serial analysis of gene expression (SAGE) libraries were generated from tubular conceptus mRNA. Comparing the three libraries at 12,000 tags/library indicated small-amplified RNA-SAGE was a reliable amplification procedure. The unamplified library was increased to 42,415 tags and statistical analyses of tag frequencies with previously generated ovoid and filamentous libraries revealed the differential expression ($P < 0.05$) of 483 and 364 tags between ovoid:tubular or tubular:filamentous libraries, respectively. Annotated transcripts known to be involved in development and also potentially regulated by estrogen (cytokeratins 8 and 18, stratifin, midkine, and glycolytic enzymes) were further analyzed by real-time PCR. The majority of glycolytic enzyme transcripts were constitutively expressed or downregulated at the filamentous stage. Likewise, cytokeratin mRNAs were less abundant in filamentous conceptuses, whereas stratifin and midkine were more abundant in tubular conceptuses. Analysis of protein revealed distinct expression patterns for cytokeratin 18, stratifin, and midkine. The function(s) of these factors and potential modulation by estrogen clearly needs to be elucidated to understand their physiological role in normal conceptus development. *Mol. Reprod. Dev. 73: 1491–1502, 2006.* © 2006 Wiley-Liss, Inc.

Key Words: peri-implantation; elongation; gastrulation; transcriptome; tubular conceptus

INTRODUCTION

Elongation of the pig conceptus during day 11 (D11) to day 12 (D12) is a critical peri-implantation period where the morphological remodeling of the trophectoderm from an ovoid (~10 mm) to dynamic intermediate tubular states, and, ultimately, a long thin filament (>150 mm) occurs. Conceptus loss during this elongation phase can approach 18% (Bennett and Leymaster, 1989). The expansion phase of the blastocyst's trophectoderm tissue during elongation is a very rapid process (30–40 mm/hr; Geisert et al., 1982; Stroband and Van der Lende, 1990; Geisert and Malayer, 2001). Cellular differentiation and remodeling rather than hyperplasia are thought to be responsible for the initial morphological transition in the pig blastocyst, and this differs from other ungulates where hyperplasia is a major component (Geisert et al., 1982; Pusateri et al., 1990; Geisert and Malayer, 2001). Asynchrony of trophectoderm elongation among porcine conceptuses is evident, and precocious progression through this period is associated with conceptus competency (Bazer et al., 1993). Beyond D12 the filamentous conceptus continues to increase in length to ~100 cm by day 16 (D16).

Divergent from humans and mice, gastrulation in porcine, ovine, and bovine conceptuses is not dependent on implantation and commences around the time of elongation (Hue et al., 2001; Flechon et al., 2004; Guillomot et al., 2004). Early stages of ED polarization in ungulates is observed by the aggregation of mesoderm-like cells towards the posterior pole. In the pig, cow, and sheep conceptuses, primordial mesoderm cells intercalate in between the embryonic disc (ED; epiblast) and endoderm (hypoblast), migrate towards the extra-embryonic regions, and split to form the yolk sac membrane by fusion with the primitive endoderm (Stroband and Van der Lende, 1990; Maddox-Hyttel

This article contains Supplementary Material available at http://www.interscience.wiley.com/jpages/1040-452x/suppmat.

Grant sponsor: USDA ARS CRIS; Grant number: 1265-31000-082.

*Correspondence to: Le Ann Blomberg, Biotechnology and Germplasm Laboratory, USDA Agricultural Research Service, Animal and Natural Resources Institute, Bldg 200, Rm 101A, BARC-East, Beltsville, MD 20705. E-mail: lblomberg@anri.barc.usda.gov

Received 30 December 2005; Accepted 12 February 2006
Published online 10 August 2006 in Wiley InterScience (www.interscience.wiley.com).
DOI 10.1002/mrd.20503

et al., 2003; Flechon et al., 2004; Guillomot et al., 2004). In conjunction with tissue differentiation, the morphology of the ED changes in sheep; the round ED becomes oblong and then pear-shaped with a tapered posterior end (Guillomot et al., 2004). Following further development, a primitive streak is established that extends from the posterior end towards the anterior region (Hue et al., 2001; Maddox-Hyttel et al., 2003; Flechon et al., 2004; Guillomot et al., 2004). Brachyury, a developmental factor with roles in embryonic mesoderm specification and body axis elongation during gastrulation, has been utilized to identify mesodermal cells localized in the posterior region of the conceptus as well as their extra-embryonic movement and the formation of the primitive streak (Beddington et al., 1992; Kispert et al., 1994; Wilson et al., 1995; Hue et al., 2001).

A well-known physiological process crucial to normal conceptus development and gestation in swine is steroid hormone synthesis. Precise production and secretion of estrogen by the conceptus, in particular during the peri-implantation period encompassing D11–D12, is important for maternal recognition of pregnancy as well as embryo viability (Perry et al., 1976; Geisert et al., 1982; Niemann and Elsaesser, 1986; Geisert et al., 1990; Pusateri et al., 1990; Geisert and Yelich, 1997). The upregulation of factors crucial for estrogen synthesis in the conceptus coincides with its peak estrogen secretion (Conley et al., 1992; Yelich et al., 1997; Blomberg and Zuelke, 2004; Blomberg et al., 2005). The administration of estrogen at certain points during the peri-implantation period and exposure of conceptuses to a more advanced uterine environment can result in conceptus loss, suggesting that the proper endocrine milieu is required for survival (Blair et al., 1991; Geisert et al., 1991). Estrogen's action on the endometrium results in the modulation of prostaglandins towards a pro-pregnancy environment and growth factor release that promotes growth of the conceptus trophectoderm (Ka et al., 2001; Jaeger et al., 2001). Furthermore, the presence of estrogen receptor beta and upregulation of mRNA by estradiol-17 beta in the conceptus indicate that estrogen synthesized by the conceptus could also have an autocrine effect (Kowalski et al., 2002).

Despite our knowledge of the requirement for distinct morphological phenotypes and specific physiological processes, little is known about the molecular mechanisms and their regulation, essential for conceptus survival during elongation. Our lab previously employed serial analysis of gene expression (SAGE) to obtain global transcriptome profiles of ovoid and filamentous porcine conceptuses, stages that precede and follow elongation, respectively (Blomberg and Zuelke, 2004). The large number of putative transcripts identified (>22,000) and their functional categorization enabled an initial assembly of potential molecular pathways existing in the conceptus.

The primary aim of this study was to elucidate the transcriptome profile of the tubular porcine conceptus so as to identify molecular pathways that enable progression through the elongation period. Of particular interest were estrogen responsive factors associated with growth, morphogenesis, and cell or tissue differentiation that might account for the phenotypic changes of the porcine conceptus. Downstream analysis examined the spatial and temporal protein expression of two potentially important development genes: stratifin (SFN) and midkine (MDK). The relative abundance of tubular RNA made possible an assessment of amplification strategies for transcriptomic analysis of conceptuses at earlier stages of development. A secondary aim was to better characterize the D11 through D12 conceptuses being utilized by examining their growth status and the developmental stage of the ED.

MATERIALS AND METHODS

Animals

Hybrid gilts 6 months of age or older with normal estrous cycle and weighing at least 100 kg were superovulated and mated using artificial insemination for in vivo conceptus production (Blomberg et al., 2005). Conceptuses undergoing elongation between gestational D11 and D12 were grouped according to morphology and size: ovoid (4–10 mm), tubular (12–80 mm), and filamentous (100–150 mm) (Blomberg et al., 2005). Ovoid and tubular conceptuses were collected individually or as pools (~5 conceptuses/pool); filamentous conceptuses were collected only as pools (~5 conceptuses/pool) to minimize handling and avoid potential tissue tears (Blomberg et al., 2005). All animal protocols were approved by the Beltsville Area Animal Care and Use Committee and meet the USDA and NIH guidelines for the care and use of animals.

Total RNA Preparation

Total RNA was isolated from pooled or individual ovoid and tubular conceptuses, as well as pooled filamentous conceptuses using, the RNAeasy Kit (Qiagen, Valencia, CA; Blomberg et al., 2005). A DNase I digest (Turbo DNA-free, Ambion, Austin, TX) of 10 μg total RNA from each conceptus sample was performed according to the manufacturer's instructions, to remove genomic DNA contaminants. Total RNA integrity and quantification were analyzed with the Agilent 2100 Bioanalyzer and RNA 6000 Nano LabChip Kit (Agilent Technologies, Palo Alto, CA).

SAGE Library Construction and Sequencing

A small amplified RNA-SAGE (SAR-SAGE) library was constructed using ~50 ng of total RNA from a pooled tubular conceptus sample according to the method of (Vilain et al., 2003; Vilain and Vassart, 2004). The T7 adapter sequence was analyzed in silico to ensure that it did not correspond to any predicted porcine tag. The I-SAGE® kit (Invitrogen, Gaithersburg, MD), based on methodology by Velculescu et al. (1995), was used for all experimental steps except mRNA T7 polymerase amplification, which was performed with the T7 Megascript kit (Ambion). Two additional SAGE libraries were

generated from either 50 ng (for PCR-amplified) or 5 μg total RNA (unamplified library). Ditag amplification was carried out for 27 cycles for SAR-SAGE (after T7 amplification) and unamplified libraries, whereas an additional eight cycles were performed for the PCR-amplified library. Amplification of SAGE concatemers, sequencing and sequence analysis were performed as described previously (Blomberg and Zuelke, 2004).

Real-Time RT-PCR

The initial total RNA template for real-time RT-PCR was derived from multiple pools of non-related ovoid, tubular, or filamentous conceptuses collected on separate days. Additionally, total RNA isolated from individual conceptuses was also analyzed: ovoid (8 mm), tubular (group 1: 12 mm; group 2:20–22 mm; group 3: 30–38 mm; and group 4: 42–52 mm). Gene-specific primers were designed from porcine-specific sequences for [*hexokinase 1* (HK1), *glyceraldehyde-3-phosphate dehydrogenase* (GAPDH), *pyruvate dehydrogenase* (PDHA1), *pyruvate kinase* (PKM2), *aldolase A* (ALDOA), *glucose phosphate isomerase* (GPI), *phosphofructokinase* (PFKP), and *lactate dehydrogenase-B* (LDHB)], *stratifin* (SFN), *midkine* (MDK), *cytokeratin 8* (KRT8), and *cytokeratin 18* (KRT18) that were obtained from GenBank. (Supplementary Table 1). Real-time PCR and statistical analysis by ANOVA were performed as described previously (Blomberg and Zuelke, 2004). Results were expressed as relative quantity (RQ) of the transcript of interest (Blomberg and Zuelke, 2004).

Western Blotting

For protein analysis, conceptuses were sorted into groups based on morphology and size. Ovoid conceptuses from two distinct size populations (8 and 10 mm) were pooled (2 conceptuses/pool). Similarly, tubular conceptuses were size sorted into two separate populations (13–15 mm and 18–19 mm). Filamentous pools (100–150 mm) consisted of ~5–6 conceptuses/pool. Western blots were performed and analyzed as previously described (Blomberg et al., 2005). Blots were initially probed with primary antibodies for KRT18 (C8541, SIGMA, St. Louis, MO; diluted 1:50,000), SFN (Abcam, Cambridge, MA; diluted to 0.5 μg/ml) and MDK (R&D Systems, Minneapolis, MN; diluted to 0.04 μg/ml) followed by a secondary antibody incubation with either HRP-labeled goat anti-mouse IgG antibody (Amersham, Arlington Heights, IL; KRT18 and SFN) or HRP-labeled rabbit anti-goat IgG (Kirkregaard and Perry Laboratories, Gaithersburg, MD; MDK).

Immunohistochemistry

Conceptuses utilized for ED staging or protein expression analysis via immunohistochemistry were rinsed in 1× phosphate buffered saline (1× PBS; AccuGENE, Rockland, ME), pH 7.4, immediately after flushing and fixed in 4% paraformaldehyde (Polyscience, Inc., Warrington, PA)/1× PBS at 22°C (room temperature) for 30 min. Fixed tissues were rinsed with 1× PBS and stored in the same buffer at 4°C. Prior to immunostaining, the ED (epiblast and hypoblast) and the immediate surrounding trophectoderm were dissected away from the bulk of the trophectoderm. Tissues sections were permeabilized in 0.3% Triton X-100 in *Tris* buffered saline (TBS; 1.5% NaCl, 50 mM *Tris*-HCl, pH 7.6) for 30 min at 22°C followed by an overnight incubation at 4°C. The next day, tissues were blocked in three 30-min washes of TBS containing 1% normal serum (TBS-S; normal goat serum for mouse-derived antibodies or normal donkey serum for goat-derived antibodies). Conceptus tissues were incubated overnight with primary antibodies for either SFN (mouse anti-human; diluted to 2 μg/ml in TBS-S), KRT18 (mouse anti-human; diluted to 1:5,000 in TBS-S), MDK (goat anti-human; diluted to 10 ng/ml in TBS-S), *brachyury* (goat anti-human, diluted to 10 ng/ml) or *Ki67* (mouse anti-human; diluted to 1:200 TBS-S; Novacastra, Burlingame, CA). Excess primary antibody was removed with four 30-min 22°C washes in TBS-S. Secondary antibodies (Molecular Probes, Eugene, OR) labeled with Alexa 594 label and Alexa 488 labeled phalloidin (Molecular Probes) were diluted 1:400 and 1:100 in TBS-S, respectively, and added to tissue sections for an overnight 4°C incubation. The subsequent day, samples were carried through three 30-min washes at 22°C: first, TBS-S; second, TBS-S containing 1,000 ng/ml DAPI; and third, TBS-S. The tissues were removed from buffer, rinsed briefly with water, and mounted on slides in ProlongGold (Molecular Probes).

RESULTS

Growth and Staging of Embryonic Disc During Elongation

Initiation and progression of gastrulation in the ED was determined in ovoid, tubular, and filamentous conceptuses by examining the expression of *brachyury*, a marker of early mesoderm. The ED displayed varying morphologies from the round to oblong disc and the more developmentally advanced pear with a tapered posterior region (Fig. 1B,D,E). Evidence of differentiated mesenchymal tissue and polarization of the ED was found by the detection of anti-*brachyury* positive cells localized to the posterior pole as well as in cells that had begun to migrate outside and away from the ED (Fig. 1A,C). At more advanced stages of gastrulation, anti-*brachyury* immunoreactivity in pear-shaped EDs was observed in the cells of the primitive streak (Fig. 1D). Interestingly, a distinct developmental state of the ED did not absolutely correspond with conceptus trophectoderm morphology. The D11 ovoid embryos contained EDs that were round, oblong, or pear-shaped. Although polarization of the ovoid EDs and extra-embryonic migration of the mesoderm was evident, none had a visible primitive streak. Among the filamentous conceptuses some round/oblong EDs were observed; however, the majority of EDs were pear-shaped. At this latter stage of development, the primitive streak had formed in some EDs. Pinpointing

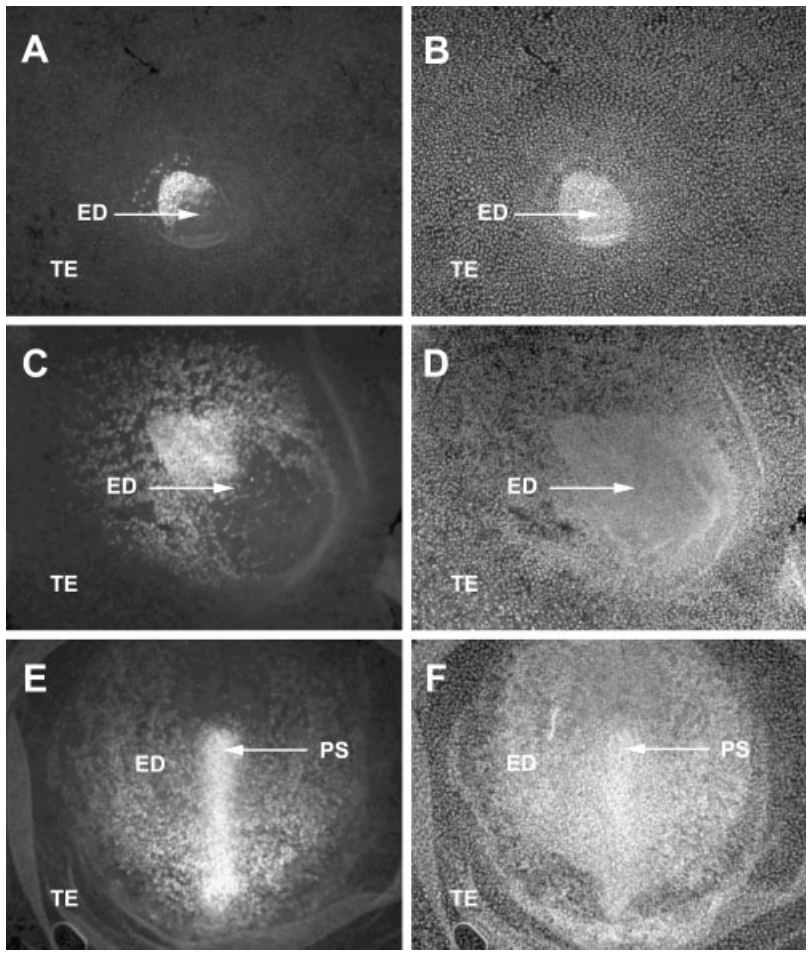

Fig. 1. Gastrulation state of the conceptus D11–D12. Expression of brachyury protein was analyzed in dissected whole mount conceptuses by immunohistochemistry. Representative results of staining patterns for brachyury in an ovoid (**A**) and two filamentous (**C** and **E**) conceptuses are depicted. Positive cells outside of the ED boundaries are mesodermal cells migrating extra-embryonically beneath the trophectoderm (TE). Nuclear staining with DAPI (**panels B**, **D**, and **F**) was carried out to determine the ED shape and the intracellular localization of brachyury. Primitive streak (PS) formation is apparent in one filamentous conceptus (**E** and **F**).

the exact gestational time necessary to obtain large numbers tubular conceptuses and populations of similar was very difficult, therefore, their gastrulation state of the tubular stage was not examined as thoroughly. Examination of the expression of other developmental factors associated with cellular differentiation within the ED, for example, *SSEA*, *vimentin*, and *Oct 3/4*, demonstrated the expected spatial and temporal expression patterns (data not shown; Flechon et al., 2004).

Besides the apparent structural changes occurring in the ED, the trophectoderm was dramatically altered during this period of time. Utilizing a marker of cell proliferation, *Ki67*, it was evident that cellular growth was a component of conceptus elongation as well as gastrulation (Fig. 2A,B). A considerable number of cells positive for *Ki67* were found dispersed throughout the trophectoderm and ED of every conceptus stage, that is, ovoid, tubular, and filamentous. In some conceptuses, a qualitative difference in the staining pattern was observed, but this was conceptus rather than stage dependent (data not shown).

Comparison of Unamplified and Amplified Libraries

One problem with doing SAGE analysis on embryos is collecting sufficient RNA for SAGE library construction; therefore, we were interested in identifying an efficient SAGE amplification procedure. Tubular conceptus libraries consisting of 12,000 tags were generated from a SAR-SAGE library, PCR-amplified library, and an unamplified standard SAGE library to test the integrity of the amplification methodologies. A comparative analysis of the frequencies of the 151 most abundant tags identified in all three libraries revealed that SAR-SAGE was a more reliable amplification method (Vilain and Vassart, 2004). Seventy-five percent of the SAR-SAGE library tags, in contrast to 43% of the PCR-amplified library tags, had less than a twofold frequency difference when compared with the unamplified library tags occurring at a frequency of at least 10. An example of the results obtained from three randomly selected high, mid, and low frequency tags are depicted in Table 1.

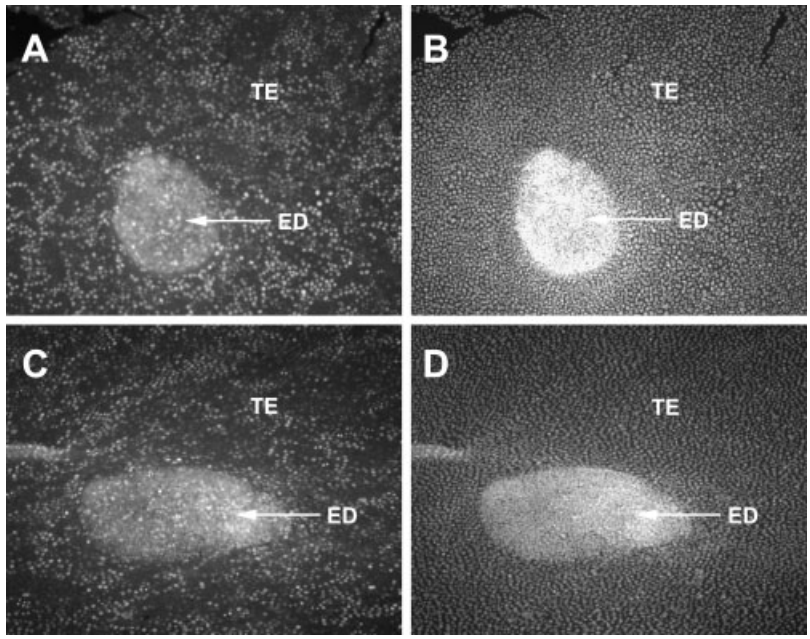

Fig. 2. Proliferative cell populations present in elongating conceptuses. Analysis of the growth status with anti-Ki67 antibody indicated that many cells throughout the ED and trophectoderm (TE) were actively proliferating: **panel A**, ovoid conceptus, *Ki67*; **panel B** ovoid conceptus, DAPI; **panel C**, tubular conceptus *Ki67*; **panel D**, tubular conceptus DAPI.

Analysis of Conceptus Transcriptomes at Different Stages of Elongation

For a more complete analysis of the tubular transcriptome profile, the unamplified tubular SAGE library was extended further to a total of 42,415 tags representing 12,777 unique putative transcripts (NCBI GEO Acc No. GSE3875). A comparison of SAGE tags and frequencies was made between the tubular SAGE library and the previously generated SAGE libraries, ovoid (42,389 tags) and filamentous (42,391 tags) (NCBI GEO Acc. No. GSE1453; Blomberg and Zuelke, 2004). Together all three libraries totaled 127,195 tags, yielding 33,191 unique tags. Interestingly, only 10.8% (3,575/33,191) of the tags were common to all three libraries. Comparisons between two libraries, ovoid:tubular or tubular:filamentous, revealed a higher degree of similarity; 22.6% (tubular vs. ovoid; 5,028/22,215) and 24.3% (tubular vs. filamentous; 5,065/20,812), consistent with the 22.5% similarity observed between ovoid and filamentous libraries previously (Blomberg and Zuelke, 2004). Statistical analysis of the tag frequencies via Chi-square with Monte–Carlo simulations revealed the greatest differential gene expression ($P < 0.05$) existed between the tubular and ovoid stages (483 tags) followed by ovoid and filamentous stages (431 tags; Blomberg and Zuelke, 2004) and finally tubular and filamentous stages (364 tags). Interestingly, across all three libraries only 35 tags had frequencies (expression levels) that were significantly different at each of the three stages examined (Table 2). Constitutive and differentially expressed SAGE tags with a frequency sum ≥ 2 in library cross comparisons were BLASTed against The Institute for Genome Research (TIGR) porcine index database (Release 11; 01-18-2005) for transcript assignment. Functional classification ensued according to gene ontology (GO) annotation appended in TIGR using the GO terms. Transcripts were designated GO terms under biological process or cellular physiological process at the fourth or fifth level.

TABLE 1. Comparison of Amplified and Unamplified Tubular Libraries

SAGE tag	SAR-SAGE tag frequency	PCR-amplified tag frequency	Unamplified tag frequency
AAGCCTGGAG	112	61*	153
GATTGTGGTA	163	80	142
GCACACTAGG	113	209	138
CAGGCCACGC	87	19*	53
CTGTACAACG	59	17*	53
TCCGTGGTTG	57	41	51
AAAAATCATC	31	13*	50
GGGTTTTTAT	11	4*	12
ATAATGATGG	16	4*	11

*Twofold different with respect to unamplified library.

A total of 681 transcripts demonstrated a statistically significant difference in expression during at least one stage of development. The types of expression patterns detected between the three stages of development are listed in Table 3. Tags with a frequency >10 in at least one library are listed in Supplementary Table 2 and are grouped according to expression profile. Of the 35 tags demonstrating differential expression across all three developmental stages, 22 (63%) matched a single unique TC (transcript), one matched multiple transcripts, and 13 had no match (Table 2). The nine tags continuously upregulated with the progression of development are

TABLE 2. Transcripts Differentially Expressed at All Stages of Elongation

SAGE Tag	Ovd freq	Tub freq	Fil freq	Transcript annotation	GO term
CTGTACAACG	49	213	177	TC221154 CYP19A	GO:0044255: cellular lipid metabolism
TGGATGATAA	118	93	238	TC219753 similar to PSAP	GO:0044255: cellular lipid metabolism
AAATAAAGAA*	3	40	83	TC220366 mGST1	GO:0051186: cofactor metabolism
GTTTTGAGTT*	3	25	48	TC200444 STAR	GO:0044255: cellular lipid metabolism
TTGTATTGTA*	66	92	130	TC201347 NDUFA4	GO:0005739: mitochondrion
GCCCTGGGGC	135	168	58	TC200713 UBA52	GO:0044249: cellular biosynthesis
AGAAATCTGA	319	68	179	TC200462 similar to KRT18	GO:0006996: organelle organization and biogenesis
TCTCCCTTTG	65	173	8	TC219411 SLC25A6	GO:0006996: organelle organization and biogenesis
CTCCCACCCC	34	75	51	TC199406 MDK	GO:0000074: regulation of progression through cell cycle
GAAGATCAAT	28	6	15	TC200994 SNX3	GO:0016192: vesicle-mediated transport
GCCCCCAATA*	31	48	73	TC219859 LGALS1	GO:0016337: cell–cell adhesion
GAAGAGGCCT	91	32	50	TC200822 similar to PRAP1	
TGCCCCTCCT*	124	211	293	TC220093 Replication protein-like	
GCCTTTAAGG	68	28	48	TC224669 ARPP-21	
GAAGTCGGAA	17	4	29	TC199620 Lepidosiren paradoxa 28S ribosomal RNA TC219434 COXI	
TCTGTATACA*	11	28	43	TC202823 similar to PKIB	
CGCCGCCGGC	48	71	21	TC200656 RPL35	
GCGAAAGGCT*	4	13	31	TC221929 similar to MGC84261 protein	
CCCATTGTAC*	375	599	660	TC219434 COXII	
TGTCATTCTG*	72	118	157	TC201484	
TATGATGACT	7	32	19	TC219114	
GGCAAGCCCC	124	174	65	Multiple TCs	
ATACATATTA	46	16	30	Unknown	
AAATACTATT	29	122	65	Unknown	
GGTGCAGGCG	5	29	15	Unknown	
CTGTGTATGC	0	21	5	Unknown	
AAAAATCATC	19	101	46	Unknown	
TCTCCCGTTT	69	43	153	Unknown	
TGCCCTCCTC	5	0	37	Unknown	
TCCCCGTACA	124	32	81	Unknown	
ATACTTGGAA	171	425	226	Unknown	
AAGGAGATGG	53	14	28	Unknown	
AGGTTGCGGG	257	81	116	Unknown	
TCCCTATTAA	227	30	113	Unknown	
GTGACCACGG	65	30	46	Unknown	

Freq, Tag frequency which reflects expression level; Ovd, ovoid; Tub, tubular; Fil, filamentous.

TABLE 3. Expression Patterns Detected During Elongation

	# of tags (transcripts) and expression pattern
Constant increase across all stages	9: Ovd < Tub < Fil
Peak expression in tubular stage	54: Tub > Ovd and Fil; Ovd = Fil
	8: Tub > Ovd and Fil; Ovd < Fil
	4: Tub > Ovd and Fil; Ovd > Fil
Nadir in tubular stage	27: Tub < Ovd and Fil; Ovd = Fil
	3: Tub < Ovd and Fil; Ovd < Fil
	10: Tub < Ovd and Fil; Ovd > Fil
Other patterns of expression	31: Ovd < Tub; Ovd = Fil; Tub = Fil
	47: Ovd > Tub and Fil; Tub = Fil
	23: Ovd = Tub; Ovd and Tub > Fil
	40: Ovd = Tub; Ovd and Tub < Fil
	59: Tub = Fil; Tub and Fil > Ovd
	39: Ovd = Tub; Tub = Fil; Ovd < Fil
	32: Ovd = Tub; Tub = Fil; Ovd > Fil
	18: Ovd = Tub; Tub < Fil; Ovd = Fil
	28: Ovd = Tub; Tub > Fil; Ovd = Fil
	31: Ovd > Tub; Tub = Fil; Ovd = Fil

Ovd, ovoid; Tub, tubular; Fil, filamentous.

highlighted by the asterisk. An examination of the annotated transcripts revealed that they encoded proteins from diverse molecular processes, such as general metabolism, cellular organization, cell cycle, and cell–cell interaction (Table 2). A total of 2,681 tags were constitutively expressed transcripts in the three SAGE libraries, and, of those, 1,069 had a unique TC match. Examination of the annotated transcripts revealed that many encoded proteins involved in general metabolic activities, such as protein, carbohydrate, amino acid, nucleic acid, and lipid metabolism. Transcripts differentially regulated at the transitional tubular stage that could potentially be regulated by estrogen, included those encoding glycolytic enzymes (HK1, PFKP, and GAPDH), cytoskeletal proteins (KRT8 and KRT18), a negative growth regulator protein (SFN) and a protein involved in embryonic neurogenesis (MDK). Considering the morphological changes occurring in the trophectoderm and ED, noteworthy was the presence of transcripts for the cell proliferation marker *Ki67*, mesoderm markers (*mesoderm development candidate 1 and 2*), an early endoderm marker (*bone morphogenetic protein 2*), and a family of proteins involved in cellular polarization (*rab* family members).

Validation of Transcript Expression

Conceptus elongation in swine is a very dynamic period in which striking changes in morphology and size occur. Transcripts encoding factors involved in energy metabolism (glycolysis), cytoskeletal architecture, cell cycle, and the differentiation or survival of specific tissue types were selected for further analysis (Table 4). Differential expression of the mRNAs identified by SAGE was examined by determining the RQ of each transcript with respect to β-actin via real-time PCR (Blomberg and Zuelke, 2004). Real-time PCR and SAGE expression patterns of glycolytic transcripts, HK1, PFKL, GAPDH, GPI, ALDOA, PKM2, and LDHB corresponded for some but not all factors (Table 4). Constitutive expression of PDH, GPI, PKM2, LDHB, and ALDOA at the different stages was confirmed for all but ALDOA. That is, with respect to the ovoid conceptus, the ALDOA transcript level was increased in both tubular and filamentous conceptuses. The HK1 mRNA, which displayed upregulation in tubular and filamentous conceptuses by SAGE, was constitutively expressed according to PCR. As per SAGE, the PFKL mRNA level was downregulated in the tubular and filamentous conceptuses; however, PCR indicated that the level was lowest in ovoid and tubular conceptuses and upregulated in the filamentous. In contrast, the differential expression pattern of GAPDH was confirmed; GAPDH levels were similar in ovoid and tubular conceptuses before decreasing in the latter filamentous stage. The PCR analysis of the expression of transcripts encoding the developmental protein MDK was in complete accordance with SAGE; peak expression was observed at the tubular stage (Table 4). On the other hand, the decrease in KRT8 and KRT18 transcript levels was evident only in the filamentous conceptuses while levels in the tubular conceptus were not significantly different from the ovoid stage (Table 4). The mRNA for SFN increased in the tubular conceptuses, in accordance with SAGE, however, in the filamentous conceptus the PCR analysis was inconsistent; SFN mRNA decreased rather than remaining elevated (Table 4). Due to our limited knowledge of the pig genome, it is unclear at this time whether the inconsistencies between PCR and SAGE are a consequence of the presence of unidentified splice variants.

Protein Expression of Developmental Genes

Transcripts encoding developmental factors that could potentially be regulated by estrogen were analyzed further at the protein level. These included KRT18, SFN, and MDK. Western blot analysis of conceptuses at various stages of elongation revealed protein for each factor was present at all ovoid, tubular,

TABLE 4. Expression Patterns of Transcripts Encoding Glycolytic Enzymes

SAGE Tag	mRNA	SAGE frequency ovd:tub:fil	Ovd RQ	Tub RQ	Fil RQ	Function
TCGTATGACC	HK1	2:15:15	0.975 ± 0.102	1.039 ± 0.24	1.188 ± 0.131	GO:0044237: cellular metabolism
CAGTGGATCA	PFKL	57:16:12	0.262 ± 0.01	0.189 ± 0.079	0.712 ± 0.176[a,b]	GO:0044237: cellular metabolism
TACCATCAAT	GAPDH	97:87:59	1.657 ± 0.144	1.397 ± 0.256	0.86 ± 0.073[a]	GO:0044237: cellular metabolism
CTATTTTTAT	PDH	0:2:3	1.092 + 0.106	0.907 ± 0.105	0.843 ± 0.099	GO:0044237: cellular metabolism
TTCACTGTTC	GPI	8:10:9	1.203 ± 0.102	1.01 ± 0.184	1.087 ± 0.273	GO:0044237: cellular metabolism
CCTACTAAGC	ALDOA	12:12:9	1.745 ± 0.326	1.097 ± 0.132	0.78 ± 0.111[a]	GO:0044237: cellular metabolism
AAGCAGTGGT	PKM2	7:0:3	0.776 ± 0.049	0.557 ± 0.08	0.725 ± 0.155	GO:0044237: cellular metabolism
CTTAGTTTAA	LDHB	20:23:26	0.649 ± 0.062	0.655 ± 0.13	0.753 ± 0.124	GO:0044237: cellular metabolism
AGAAATCTGA	KRT18	319:68:179	1.00 ± 0.129	0.963 ± 0.234	0.497 ± 0.087[a]	GO:0016043: cell organization/biogenesis
AGTATCCACA	KRT8	209:98:104	0.917 ± 0.042	0.837 ± 0.189	0.366 ± 0.035[a,b]	GO:0016043: cell organization/biogenesis
TTTCCTCTCA	SFN	72:192:225	1.037 ± 0.055	2.832 ± 0.644[c]	1.383 ± 0.329[b]	GO:0008283: cell proliferation
CTCCCACCCC	MDK	34:75:51	1.152 ± 0.12	2.227 ± 0.119[c]	1.331 ± 0.073[b]	GO:0008283: cell proliferation

[a]Ovoid versus filamentous.
[b]Filamentous versus tubular.
[c]Tubular versus filamentous and ovoid.

and filamentous stages examined (Fig. 3). Protein for MDK (~13 kDa) was detected in all samples at each stage and variations in protein level were only among samples and not developmental stage (Fig. 3A). The expected 50 kDa KRT18 protein along with a slightly smaller protein of 45 kDa was detected in almost all conceptuses examined (Fig. 3B). At the filamentous stage there appeared to be less KRT18 protein overall, and, with increased protein loading, the smaller protein product was also evident (data not shown). Developmental differences in expression pattern were clear with SFN; a protein product of ~32 kDa (+10%) was evident in ovoid and tubular conceptuses, however, by the filamentous stage a second protein product of ~29 kDa (+10%) became apparent (Fig. 3C).

An investigation into the temporal and spatial expression of KRT18, SFN, and MDK was carried out by immunohistochemistry on whole mount conceptuses. The expression of KRT18 was confined to the trophectoderm and localized to cytoskeleton (Fig. 4A). Likewise, SFN protein was present only in the trophectoderm, but there was an obvious difference in the staining intensity in the filamentous conceptus. Compared with the ovoid conceptus where SFN immunostaining was diffuse and quite uniform; distinct populations of cells in the filamentous conceptus highly expressed SFN, and the protein was present predominantly within the cytoplasm (Fig. 4B). However, in certain cells nuclear localization was observed (Fig. 4B). Expression of MDK was detected in both the ED and trophectoderm. Typically, ovoid conceptuses of 8 mm contained a greater number of cells with intense cytoplasmic MDK immunostaining in trophectoderm and ED than smaller ovoid (4 mm), tubular, or filamentous conceptuses. Overall, the cytoskeletal localization of MDK predominated in the trophectoderm, but certain cell populations were present that exhibited increased cytoplasmic and/or nuclear expression (Fig. 4C,D,E). Nuclear localization of MDK was not observed in cells of the ED. Many tubular conceptuses also displayed an aggregation of cells highly expressing MDK in the cytoplasm at or close to the tips of the elongating trophectoderm (Fig. 4F).

DISCUSSION

The pig conceptus undergoes a dramatic morphological change between D11 and D12 that involves the elongation of the extra-embryonic trophectoderm as well as gastrulation within the epiblast tissue of the ED. Asynchrony of trophectoderm elongation and ED differentiation was evident in ovoid, tubular, and filamentous conceptuses; neither morphology nor size of the trophectoderm was indicative of the extent to which the ED disc had proceeded through gastrulation. The gross morphology of the ED observed in D11 and D12 pig conceptuses was similar to that found in the ovine conceptus ED between D11 and D14 (Guillomot et al., 2004). The rapid transformation of the conceptus trophectoderm from an 8 mm ovoid structure to a 100 mm filamentous structure has generally been

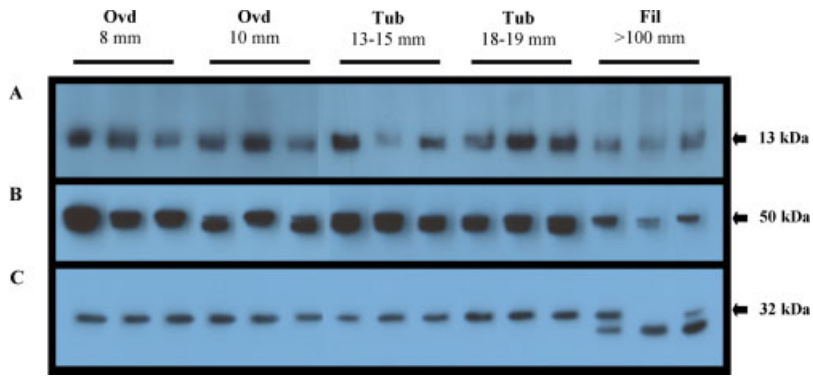

Fig. 3. Protein expression of developmental genes. Western blotting of pooled conceptuses at different developmental states, based on trophectoderm morphology, was carried out with anti-MDK (**A**), anti-KRT18 (**B**), anti-SFN (**C**). Ovoid embryos (ovd; 8 mm), tubular conceptuses (tub; 13–15 and 18–19 mm), and filamentous conceptuses (fil; >100 mm). Conceptus samples represent three independent conceptus pools (ovd and tub = 2 conceptuses/pool; filamentous ~5 conceptuses/pool). Arrows highlight protein product band of the predicted size; an additional band was observed for both KRT18 and SFN. [See color version online at www.interscience.wiley.com.]

considered to be primarily the consequence of cellular differentiation and migration (Geisert et al., 1982; Pusateri et al., 1990). However, the expression of Ki67, a protein ubiquitously expressed during the G1, S, and G2 phases of the cell cycle but not the G0 phase (resting), indicated that cell division was active within the trophectoderm and ED compartments during elongation at D11 through D12. Significant correlation between Ki67 protein expression and DNA replication via BrdU labeling indicate the utility of Ki67 as a predictor of cell proliferation and tissue growth (Muskhelishvilli et al., 2003).

Distinct transcriptome profiles were identified by SAGE at the discrete morphological stages (ovoid, tubular, and filamentous) occurring during the 24-hr period between D11 and D12 that encompasses conceptus elongation. Less that 11% of the SAGE tags (putative transcripts) were common to all three stages indicating that a large number of putative transcripts were either unique to the stage of development or not detected because of their rarity or the library size. Furthermore, comparative analysis of the total number of tags differentially expressed indicated that ovoid: tubular (483 tags) stages of development were more dissimilar followed by ovoid:filamentous (431 tags) and tubular:filamentous (364 tags). The tubular stage is a very transient stage, described as lasting ~4 hr (Geisert et al., 1982). The need for rapid and dramatic remodeling of the pig tubular conceptus morphology in this short time may require a profound change in gene expression. Genes involved in numerous physiological processes were identified by SAGE, and inclusion of the tubular stage permitted the identification of expression patterns altered within the elongation process (Table 2). Since we are interested in factors that may modulate the rapid morphological alteration of the conceptus, we further examined the expression profile of genes involved in energy metabolism, growth, cytoskeletal structure, and tissue differentiation that could potentially be regulated by estrogen.

Glycolysis in the preimplantation conceptus at early developmental stages is important for energy production; however, some of the key enzymes or metabolites have important roles in other cellular processes as well (Swain et al., 2002). For example, GPI has cytokine-like activities that are mitogenic and promote differentiation (Yanagawa et al., 2005). Key enzymes of the glycolytic pathway can be regulated either positively or negatively by estrogen in tissues including the conceptus (Nieder and Weitlauf, 1984; Gupta et al., 1989). In mice, an estrogen deficit results in delayed implantation and a downregulation of glycolysis that can be rescued upon the administration of the hormone (Nieder and Weitlauf, 1984). Confirmation of the mRNA expression profiles of glycolytic enzymes identified by SAGE indicated that most, including the key rate-limiting enzyme, HK1, are constitutively expressed or downregulated. The exception was PKFL which was upregulated at the filamentous stage. Whether the secretion of estrogen by the conceptus during this developmental period has an effect on the transcription of the glycolytic factors is unclear. However, if the expression pattern of glycolytic transcripts reflect their protein level, increased anaerobic energy production is not required during elongation.

Tissue differentiation and cellular migration within the trophectoderm and ED are important during the period of development examined in this study. Considering our limited knowledge of estrogen's autocrine effect on the conceptus, transcripts that could potentially be regulated by estrogen and modulate important developmental processes, KRT18, SFN, and MDK, were examined in greater detail. It is well known that KRT8 and KRT18 are the first types of cytokeratin found in the differentiating trophectoderm of mice. Furthermore, the type I cytokeratin 19 (KRT19) and KRT18 are crucial for normal placentation in mice and their deletion is lethal (Hesse et al., 2000). In certain cell types estrogen can modulate the arrangement of keratin intermediate filaments thus affect cytoskeletal

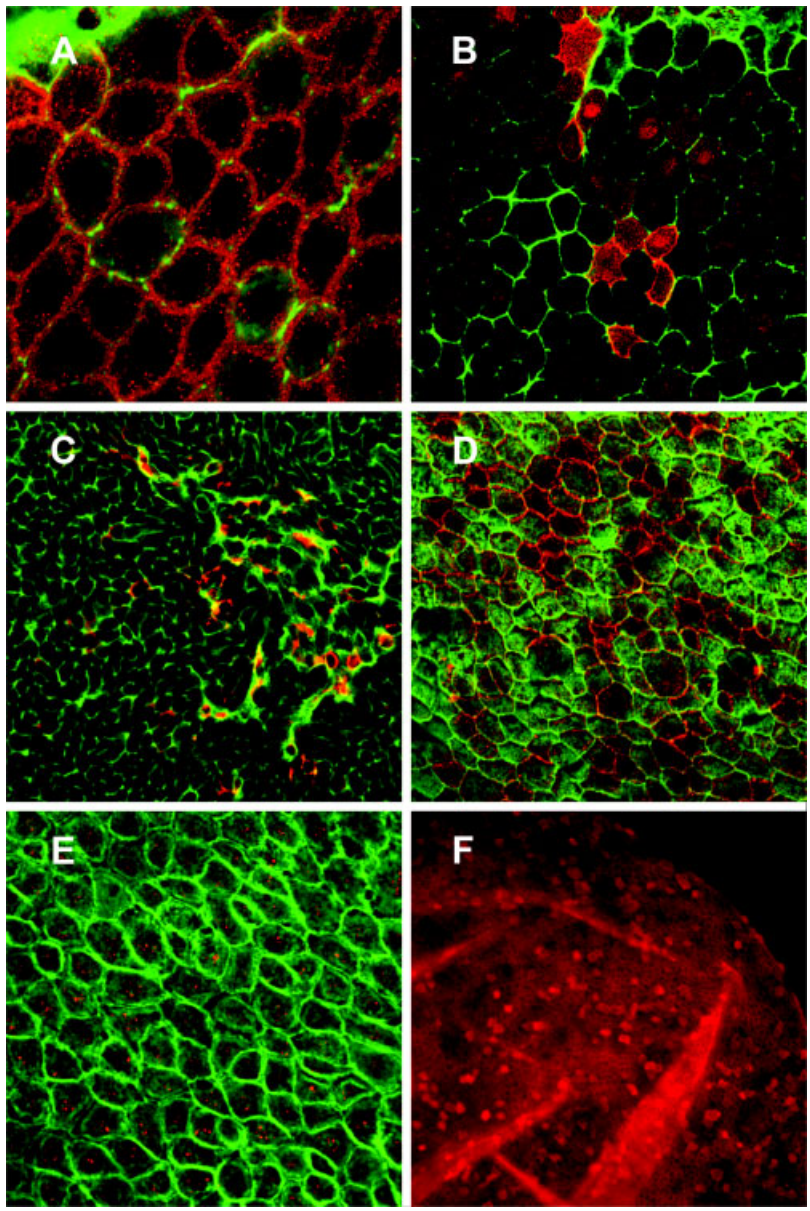

Fig. 4. Spatial and intracellular localization of developmental proteins. The distribution of MDK, KRT18, and SFN in ovoid, tubular, and filamentous conceptuses was examined by immunohistochemistry with antibodies for those antigens. The cellular localization determined by staining pattern of specific antibodies (red) is depicted: KRT18 (**A**, cytoskeletal), SFN (**B**, cytoplasmic and nuclear), MDK (**C**, cytoplasmic; **D**, cytoskeletal; **E**, nuclear; **F**, concentration of cells with cytoplasmic staining at tubular tip). Cellular F-actin in the cytoskeleton was identified with phalloidin (green). [See color version online at www.interscience.wiley.com.]

structure (Sapino et al., 1986). The KRT18 protein was expressed exclusively throughout the trophectoderm at the three conceptus stages and indicates that KRT18 plays an important role in the development of the trophectoderm.

The SFN protein belongs to a family of related but very distinct proteins involved in different cellular processes, for example, p53-dependent or -independent regulation the cell cycle, mitogen activated protein kinase cell growth, and β1-integrin directed cell migration or spreading (Mhawech, 2005). Interestingly, in some cell types KRT18 interacts with SFN and promotes the translocation of SFN from the cytoplasm to nucleus resulting in p53-dependent cell cycle arrest and cellular quiescence (Ku et al., 2002). Known as a human epithelial cell marker, SFN protein was confined to the trophectoderm along with KRT18 in the current study (Nakajima et al., 2003). Although the cytoskeletal distribution of KRT18 seemed to be quite uniform throughout the trophectoderm, SFN protein was more highly expressed in distinct trophectoderm cell populations at the filamentous stage and nuclear translocation was apparent in some cells. Whether nuclear localization was driven by SFN interaction with KRT18, and those cell populations were quiescent, remains to be determined. Furthermore, SFN can be regulated post-

translationally through the estrogen-induced zinc finger protein (EFP), which targets SFN for degradation (Urano et al., 2002). The appearance of a secondary lower molecular weight protein in the D12 filamentous conceptus raises questions of whether (1) its coincidence with peak estrogen secretion indicates EFP directed site-specific proteolysis of the protein, (2) an undescribed post-translational modification is occurring, or (3) the product of an unidentified SFN transcript variant is being expressed.

The MDK protein is a developmentally regulated heparin binding cytokine that is induced by retinoic acid, an important embryonic morphogen, which is of interest considering the developmental state of the elongating conceptus (Schweigert et al., 2002; Quadro et al., 2005). Furthermore, MDK is a ligand for several diverse cell membrane receptors that mediate different intracellular signaling pathways (Takada et al., 1997; Nakanishi et al., 1997; Shibata et al., 2002; Stoica et al., 2002). The cellular localization, cell membrane, cytoplasm, or nucleus also has a role in the multifunctional activities of MDK (Nakanishi et al., 1997; Takada et al., 1997; Shibata et al., 2002; Stoica et al., 2002). The activity of MDK protein has been associated with promoting neuronal outgrowth or survival in embryos and modulation of mesoderm formation (Rauvala, 1989; Yokota et al., 1998). It also enhances angiogenesis in tumors and hematopoetic cell migration during in the inflammatory responses (Muramatsu et al., 1993; Takada et al., 1997; Stoica et al., 2002). Interestingly, estrogen's modulation of a pro-angiogenesis response in breast epithelia appears to involve MDK as well as other well-known angiogenic factors (Zhang et al., 1995). Differences in the spatial and intracellular expression patterns of MDK protein throughout the conceptus suggested that it may have multiple roles during elongation. In the majority of cells throughout the trophectoderm, MDK protein was localized to the cytoskeleton; however, a few cells showed intense cytoplasmic staining. It will be of interest to determine whether those cell populations had an increased production or sequestration of MDK. Of particular interest was the phenomenon of MDK positive cells seeming to aggregate at the tips of the elongating trophectoderm in tubular conceptuses. The expression of MDK in the conceptus has been typically associated with neurogenesis; however, the presence of MDK in the trophectoderm suggests that it may also have a role (e.g., cellular migration) in the development of the extra-embryonic tissue as well.

Comprehensive trancriptome analysis of the tubular conceptus by SAGE has allowed the identification of factors altered within the peri-implantation elongation period of the porcine conceptus development. Furthermore, we have adapted the use of SAR-SAGE for use with porcine-derived tissue and shown that it was a more reliable method when sample amplification is required. This finding should impact future analyses of earlier stages of conceptus development, which would typically require the collection of hundreds of embryos or oocytes. Our results indicate that glycolytic factors required for energy metabolism, and potentially other important cellular processes, are not upregulated during the rapid morphological change. Furthermore, we have described the expression patterns and distribution of two potentially important estrogen-responsive developmental genes, SFN and MDK that have not been previously characterized in the porcine conceptus. Confinement of SFN expression to the trophectoderm indicates that SFN might serve as an epithelial cell marker during this period development. The expression of MDK in the conceptus trophectoderm indicates MDK has a function beyond neurogenesis in the porcine conceptus. Clearly, additional studies will need to be performed in order to ascertain the exact functions of these molecules during elongation. Their potential modulation by estrogen may enhance our understanding of the physiology of normal conceptus development and the autocrine effects of estrogen.

ACKNOWLEDGMENTS

The author thanks Lori Schreier and Jane McDougal for assistance with animal management, DNA sequencing, and immunohistochemistry, Larry Shade for bioinformatics assistance, Dr. Dave Guthrie for statistical analysis, and Dr. Neil Talbot and Dr. Rebecca Krisher for reviewing the manuscript.

REFERENCES

Bazer FW, Geisert RD, Zavy MT. 1993. Fertilization, cleavage, and implantation. In: Hafez ESE, editor. Reproduction in farm animals, 6th edition Philadelphia, Pennsylvania: Lea and Febiger. pp 88–212.

Beddington RS, Rashbass P, Wilson V. 1992. Brachyury-a gene affecting mouse gastrulation and early organogenesis. Dev Suppl: 157–165.

Bennett GL, Leymaster KA. 1989. Integration of ovulation rate, potential embryonic viability and uterine capacity into a model of litter size in swine. J Anim Sci 6:1230–1241.

Blair RM, Geisert RD, Zavy MT, Yellin T, Fulton RW, Short EC. 1991. Endometrial surface and secretory alterations associated with embryonic mortality in gilts administered estradiol valerate on days 9 and 10 of gestation. Biol Reprod 44:1063–1079.

Blomberg LA, Zuelke KA. 2004. Serial analysis of gene expression (SAGE) during porcine embryo development. Reprod Fert Dev 16:87–92.

Blomberg LA, Long LL, Sonstegard TS, Van Tassell CP, Dobrinsky JR, Zuelke KA. 2005. Serial analysis of gene expression (SAGE) during elongation of peri-implantation porcine embryos. Physiol Genomics 20:188–194.

Conley AJ, Christenson RK, Ford SP, Geisert RD, Mason JI. 1992. Steroidogenic enzyme expression in porcine conceptuses during and after elongation. Endocrinology 131:896–902.

Flechon JE, Degrouard J, Flechon B. 2004. Gastrulation events in the prestreak pig embryo: Ultrastructure and cell markers. Genesis 38:13–25.

Geisert RD, Malayer JR. 2001. Implantation. In: Hafez ESE, Hafez B, editors. Reproduction in farm animals, 7th edition Philadelphia, Pennsylvania: Lippincott, Williams and Wilkins. pp 126–139.

Geisert RD, Yelich JV. 1997. Regulation of conceptus development and attachment in pigs. J Reprod Fertil Suppl 52:133–149.

Geisert RD, Brookbank JW, Roberts RM, Bazer FW. 1982. Establishment of pregnancy in the pig. II. Cellular remodeling of the porcine blastocyst during elongation on day 12 of pregnancy. Biol Reprod 27:941–955.

Geisert RD, Morgan GL, Zavy MT, Blair RM, Gries LK, Cox A, Yellin T. 1991. Effect of asynchronous transfer and oestrogen administration

on survival and development of porcine embryos. J Reprod Fertil 93:475–481.

Geisert RD, Zavy MT, Moffatt RJ, Blair RM, Yellin T. 1990. Embryonic steroids and the establishment of pregnancy in pigs. J Reprod Fertil Suppl 40: 293–305.

Guillomot M, Turbe A, Hue I, Renard JP. 2004. Staging of ovine embryos and expression of the T-box genes Brachyury and Eomesodermin around gastrulation. Reproduction 127:491–501.

Gupta G, Srivastava A, Setty BS. 1989. Effect of antiandrogens on some key enzymes of glycolysis in epididymis and ventral prostate of rat. Indian J Exp Biol 27:324–328.

Hesse M, Franz T, Tamai Y, Taketo MM, Magin TM. 2000. Targeted deletion of keratins 18 and 19 leads to trophoblastic fragility and early embryonic lethality. EMBO J 19:5060–5070.

Hue I, Renard JP, Viebahn C. 2001. Brachyury is expressed in gastrulating bovine embryos well ahead of implantation. Dev Genes Evol 211:157–159.

Jaeger LA, Johnson GA, Ka H, Garlow JG, Burghardt RC, Spencer TE, Bazer FW. 2001. Functional analysis of autocrine and paracrine signaling at the uterine-conceptus interface in pigs. Reprod Suppl 58:191–207.

Ka H, Jaeger LA, Johnson GA, Spencer TE, Bazer FW. 2001. Keratinocyte growth factor is up-regulated by estrogen in the porcine uterine endometrium and functions in trophectoderm cell proliferation and differentiation. Endocrinology 142:2303–2310.

Kispert A, Hermann B. 1994. Immunohistochemical analysis of the brachyury protein in wild-type and mutant mouse embryo. Dev Biol 161:179–193.

Kowalski AA, Graddy LG, Vale-Cruz DS, Choi I, Katzenellenbogen BS, Simmen FA, Simmen RC. 2002. Molecular cloning of porcine estrogen receptor-beta complementary DNAs and developmental expression in periimplantation embryos. Biol Reprod 66:760–769.

Ku NO, Michie S, Ressureccion EZ, Broome RL, Omary MB. 2002. Keratin binding to 14-3-3 proteins modulates keratin filaments and hepatocyte mitotic progression. Proc Natl Acad Sci USA 99:4374–4378.

Maddox-Hyttel P, Alexopoulos NI, Vajta G, Lewis I, Rogers P, Cann L, Callesen H, Tveden-Nyborg P, Trounson A. 2003. Immunohistochemical and ultrastructural characterization of the initial post-hatching development of bovine embryos. Reproduction 125: 607–623.

Mhawech P. 2005. 14-3-3 proteins-an update. Cell Res 15:228–236.

Muramatsu H, Shirahama H, Yonezawa S, Maruta H, Maramatsu T. 1993. Midkine, a retinoic acid-inducible growth/differentiation factor: Immunochemical evidence for the function and distribution. Dev Biol 159:392–402.

Muskhelishvilli L, Latendresse JR, Kodell RL, Henderson EB. 2003. Evaluation of cell proliferation in rat tissues with BrdU, PCNA, Ki-67 (MIB5) immuno-histochemistry and in situ hybridization for histone mRNA. J Histochem Cytochem 51:1681–1688.

Nakajima T, Shimooka H, Weixa P, Segawa A, Motegi A, Jian Z, Masuda N, Ide M, Sano T, Oyama T, Tsukagoshi H, Hamanaka K, Maeda M. 2003. Immunohistochemical demonstration of 14-3-3σ protein in normal human tissues and lung cancers, and the preponderance of its strong expression in epithelial cells of squamous cell lineage. Path Int 53:353–360.

Nakanishi T, Kadomatsu K, Okamoto T, Ichihara-Tanaka K, Kojima T, Tomoda Y, Muramatsu T. 1997. Expression of syndican-1 and -3 during embryogenesis of the central nervous system in relation to binding with midkine.

Nieder GL, Weitlauf HM. 1984. Regulation of glycolysis in the mouse blastocyst during delayed implantation. J Exp Zool 231:121–129.

Niemann H, Elsaesser F. 1986. Evidence for estrogen-dependent blastocyst formation in pig. Biol Reprod 35:10–16.

Perry JS, Heap RB, Amoroso EC. 1973. Steroid hormone production by pig blastocysts. Nature 245:45–47.

Pusateri AE, Rothschild MF, Warner CM, Ford SP. 1990. Changes in morphology, cell number, cell size and cellular estrogen content of individual littermate pig conceptuses on days 9 to 13 of gestation. J Anim Sci 68:3727–3735.

Quadro L, Hamberger L, Gottesman ME, Wang F, Colantuoni V, Blaner WS, Mendelsohn CL. 2005. Pathways of vitamin A delivery to the embryo: Insights from a new tunable model of embryonic A deficiency. Endocrinology 146:4479–4490.

Rauvala H. 1989. An 18-kd heparin-binding protein of developing brain that is distinct from fibroblast growth factors. EMBO J 8:2933–2941.

Sapino A, Pietribiasi F, Bussolati G, Marchisio PC. 1986. Estrogen-and tamoxifen-induced rearrangement of cytoskeletal and adhesion structures in breast cancer MCF-7 cells. Cancer Res 46:2526–2531.

Schweigert FJ, Siegling C, Tzimas G, Seeger J, Nau H. 2002. Distribution of endogenous retinoids, retinoid binding proteins (RBP, CRABPI) and nuclear X receptor beta (RXRbeta) in the porcine embryo. Reprod Nutr Dev 42:285–294.

Shibata Y, Muramatsu T, Hirai M, Inui T, Kimura T, Saito H, McCormick LM, Bu G, Kadomatsu K. 2002. Nuclear targeting by the growth factor midkine. Mol Cell Biol 22:6788–6796.

Stoica GE, Kuo A, Powers C, Bowden ET, Buchert Sale E, Riegel AT, Wellstein A. 2002. Midkine binds to anaplastic lymphoma kinase (ALK) and acts as a growth factor for different cell types. J Biol Chem 277:35990–35998.

Stroband HW, Van der Lende T. 1990. Embryonic and uterine development during early pregnancy in pigs. J Reprod Fert Supp 40:261–277.

Swain JE, Bormann CL, Clark SG, Walters EM, Wheeler MB, Krisher RL. 2002. Use of energy substrates by various stage preimplantation pig embryos produced in vivo and in vitro.

Takada T, Toriyama K, Muramatsu H, Song XJ, Torii S, Muramatsu T. 1997. Midkine, a retinoic acid-inducible heparin-binding cytokine in inflammatory responses: chemotactic activity to neutrophils and association with inflammatory synovitis. J Biochem (Tokyo) 122(2): 453–458.

Urano T, Saito T, Tsuki T, Fujita M, Hosoi T, Muramatsu M, Ouchi Y, Inoue S. 2002. Efp targets 14-3-3σ for proteolysis and promotes breast tumor growth. Nature 417:871–875.

Velculescu VE, Zhang L, Vogelstein B, Kinzler KW. 1995. Serial analysis of gene expression. Science 270:484–487.

Vilain C, Vassart G. 2004. Small amplified RNA-SAGE. Methods Mol Biol 258:135–152.

Vilain C, Libert F, Venet D, Costagliola S, Vassart G. 2003. Small amplified RNA-SAGE: an alternative approach to study transcriptome from limiting amount of mRNA. Nucleic Acids Res 31:e24.

Wilson V, Manson L, Skarnes WC, Beddington RS. 1995. The T gene is necessary for normal mesodermal morphogenetic cell movements during gastrulation. Development 121:877–886.

Yanagawa T, Funasaka T, Tsutsumi R, Raz T, Tanaka N, Raz A. 2005. Differential regulation of phosphoglucose isomerase/autocrine motility factor activities by protein kinase CK2 phosphorylation. J Biol Chem 280:10419–10426.

Yelich JV, Pomp D, Geisert RD. 1997. Ontogeny of elongation and gene expression in the early developing porcine conceptus. Biol Reprod 57:1256–1265.

Yokota C, Takahashi S, Eisaki A, Asashima M, Akhter S, Muramatsu T, Kadomatsu K. 1998. Midkine counteracts the active signal in mesoderm induction and promotes neural formation. J Biochem (Tokyo) 123:339–346.

Zhang L, Rees MC, Bicknell R. 1995. The isolation and long-term culture of normal endometrial epithelium and stroma. Expression of mRNAs for angiogenic polypeptides basally and on oestrogen and progesterone challenges. J Cell Sci 108:323–331.